NIRSとは

1．NIRSの原理

NIRSとは，近赤外線(光)を用いて生体のヘモグロビン濃度を計測することで局所の血液量を推定し，測定部位の機能を検討する方法論である．日本語では，“近赤外線(光)スペクトロスコピー”，“近赤外分光法”などとされることが多い．

近赤外線には生体をある程度は透過し，ヘモグロビンにより吸収されるという特徴がある．パルスオキシメータは指についてのその透過光を利用することで，動脈血の酸素飽和度を測定する．頭部について散乱光を利用すると，頭表から2〜3 cmの範囲の血液量(近似的には血流量)が測定できるので，大脳皮質の活動を捉えることができる．これがNIRSである．“光トポグラフィー検査”は，頭部用NIRSの保険収載検査名である．NIRSを含めて，光を利用して脳機能を測定する方法論を“光脳機能イメージング”と総称する．

2．NIRSの特徴

NIRSをfunctional MRI(fMRI)などの他の脳機能画像検査と比較すると，①測定の対象が大脳皮質のみで深部脳構造のデータが得られない，②空間分解能がおよそ2 cmで脳回程度である，③ヘモグロビン濃度の絶対値が得られない，という短所がある一方で，④光を用いるため完全に非侵襲的なので繰り返しての検査ができる，⑤座位など自然な状況で検査ができるので日常生活に近い状態の脳機能を明らかにできる，⑥発話や運動を行いながら検査ができるので刺激処理(入力)だけでなく反応行動(出力)に伴う脳機能を検討しやすい，⑦時間分解能が高いので脳機能の時間的な変化を捉えられる，⑧装置が小型で移動可能であり検査場所の制約が少ない，⑨装置が安価でランニングコストも低廉である，という長所がある．

こうした特徴は，「自然な状態の被検者の大脳皮質の賦活反応性の時間経過を，非侵襲的で簡便に全体として捉えることができる検査」とまとめられ，内科における超音波のような位置づけの検査と言える．こうしたデータの厳密性や定量性についての限界を踏まえた利用が望ましい．NIRS測定に用いられているレーザあるいは発光ダイオードによる近赤外線は，曇天時の太陽光の1/3程度のエネルギーであり，長時間や反復しての検査でも安全性に問題はない．

3．NIRSで得られるデータ

NIRSで得られるデータは，近赤外線が生体内を通過した距離(光路長)と，通過部位におけるヘモグロビン濃度の積である(光路長濃度積)．光路長をほぼ一定と仮定して簡便にヘモグロビン濃度と略称することが多く，酸素化ヘモグロビン濃度(oxy-Hb)と脱酸素化ヘモグロビン濃度(deoxy-Hb)，および両者を合計した総ヘモグロビン濃度(total-Hb)が測定できる．

これらのデータは，近赤外線の入射ファイバーと検出ファイバーの間隔を3 cm程度とした場合には，両者を結ぶバナナ状の領域の平均値を示す．頭皮や頭蓋骨の血液量が変化しない場合には，およそ大脳皮質におけるヘモグロビン濃度の変化を反映するので，その部位の脳血液量の変化の指標であり，脳血流量とおおむね一致する．fMRIのBOLD(blood oxygenation level dependent)信号が主に細静脈のdeoxy-Hbを反映するとされるのに対し，NIRSのデータは主に毛細血管のヘモグロビンを反映するとされる．脳機能の指標としては，oxy-Hbを用いることが多い．

4．精神疾患の脳機能測定における意義

座位などの自然な姿勢で発声や運動を行いながら検査ができるというNIRSの特徴は，被検者の負担や苦痛が少ないというだけでなく，脳機能測定にとって本質的な意味がある．精神機能のうち特に情意の機能や，精神疾患における抑うつ気分・不安・幻覚などの自覚症状(体験症状)は，検査の際の姿勢や動きにより大きな影響を受けると予想できる．日常生活に近い自然な状況で検査を行うことのできるNIRSは，こうした情意の機能や自覚症状の脳機能を検討するために適している．

NIRSは，装置の開発においてわが国の医療機器企業が世界に先行しているため，精神疾患についての臨床応用としての承認もわが国の先進医療が初めてである．また研究においても，精神疾患についての英文原著論文およそ90編の2/3近くは日本発であり，わが国から世界に発信できる医療技術となっている．

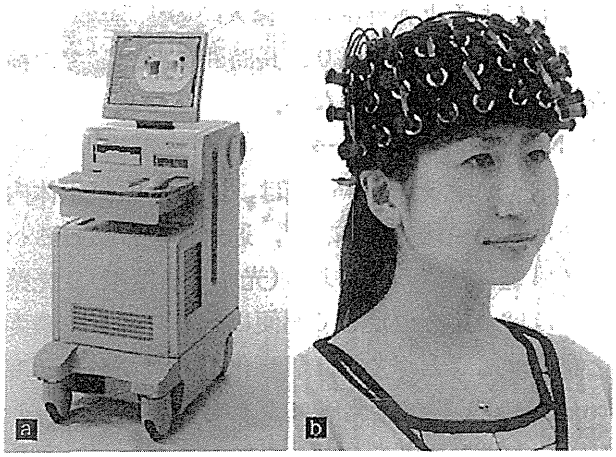

図1　NIRS 装置(a)とプローブ(b)

光トポグラフィー検査の実際

1．先進医療としての光トポグラフィー検査

NIRS 検査は 2002 年より保険収載されており(D 236-2 光トポグラフィー 670 点),「言語野関連病変(側頭葉腫瘍等)又は正中病変における脳外科手術に当たり言語優位半球を同定する必要がある場合」,「難治性てんかんの外科的手術に当たりてんかん焦点計測を目的に行われた場合」が適用となっている.

精神疾患については,2009 年に「光トポグラフィー検査を用いたうつ症状の鑑別診断補助」として,精神医療分野で初めて厚生労働省から先進医療の承認を受けた.名称にあるように,“鑑別診断補助”を目的とする検査である.精神医療の専門家にとって,精神疾患の診断では臨床症状と病歴の詳細な聴取と評価が基本となることは大前提であるが,検査を希望する当事者や家族から過大な期待を寄せられることが多いので,“補助”という言葉の意味について十分な説明が必要である.

2．先進医療の適応と施設基準

先進医療の適応となるのは,①うつ症状を呈している,②ICD-10 の F 2(統合失調症圏)または F 3(気分障害圏)が強く疑われる,③脳器質的疾患に起因するものではない,の 3 条件を満たす場合である.先進医療の実施のための施設基準として,医師については精神科・心療内科で 5 年以上の経験がある精神保健指定医,保険医療機関については神経内科または脳神経外科の常勤医と臨床検査技師がおり,医療機器保守管理体制・倫理委員会・医療安全管理委員会があることなどが条件となっている.2011 年 9 月末現在で 13 施設が承認を得ており,13,000 円程度で実施している場合が多い.

3．検査装置と検査環境(図 1, 2)

先進医療の実施には,医療器具として薬事承認された多チャンネルの NIRS 装置が必要である.52 チャンネルの NIRS 装置の場合には,光ファイバーを 3×11 に配置した測定用プローブを,左右対称で最下列が脳波記録国際 10-20 法の T_3-Fz-T_4 のラインに一致するように設置する.T_3-T_4 および T_3-Fz の距離を記録し,NIRS チャンネルと標準脳の対応を頭囲により補正する際に利用する.

測定中にプローブがずれて動くことのないよう,また近赤外線の入射と検出ファイバーが皮膚に密着するように,適度な強さで固定する.脳波の電極のように記録のためのペーストは不要なので,プローブの装着は脳波よりはるかに容易である.ただ,ファイバーと皮膚の間に頭髪が挟まると光が吸収されるので,その部分の髪はかき分ける.

検査に用いる部屋は,一般的な昼光で,できるだけ防音されていることが望ましい.NIRS 装置は被検者の後方になるように設置し,検査者は被検者の体動を視認でき,かつ被検者の視界に入りにくい位置に立つ.検査用の椅子は,体動によるアーティファクト混入を減らすためにヘッドレストと肘掛を備えたものとし,また検査を通して疲れや痛みが生じないようにリクライニング機構があるとよい.被検者前方のディスプレイに「+」マークを呈示して,頭部や眼球の動きをなるべく少なくする.

頭部の動きや体動などがあると,記録にアーティファクトが混入するので,被検者に協力を依頼する.また,検査中は被検者を観察して,アーティファクトの原因となる体動の有無を確認する.アーティファクトの混入のために測定をやりなおす場合は,再測定までに 10 分程度は間隔を空けることが好ましい.

4．言語流暢性課題

検査に用いる課題は,前頭葉機能検査として一

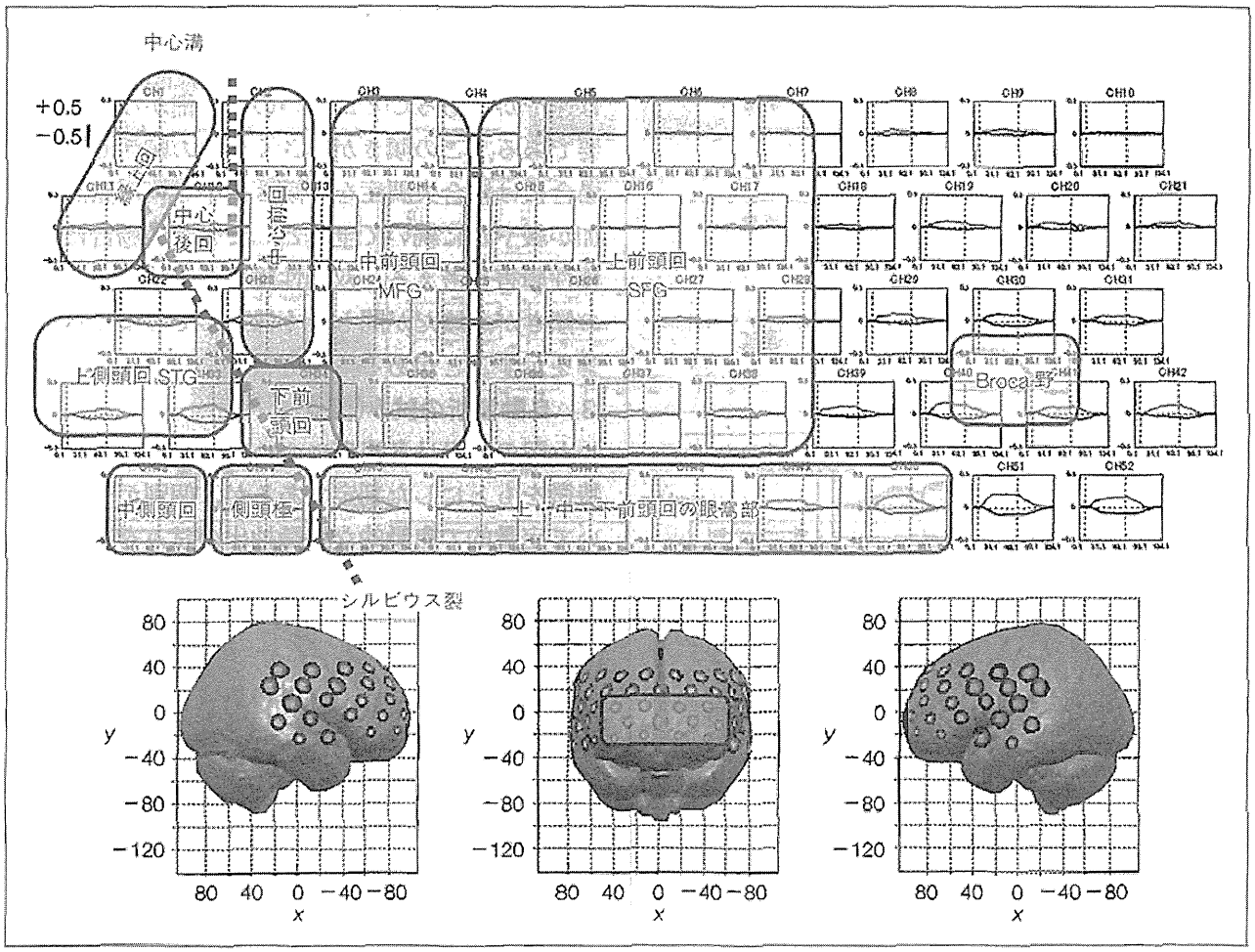

図2　NIRS チャンネルと脳構造の対応

般に用いられる言語流暢性課題(letter fluency)をNIRS測定用に修正したものである．この課題では，指定した頭文字で始まる言葉をなるべく数多く言うように求める．課題を自動提示できる装置もある．

まず，「始め，あいうえお」という音声指示により，「あいうえお」の発声を30秒間繰り返す．これは，ベースラインで無意味音を反復することで，発声による脳賦活の影響を除いたデータを得るための方法である．

次に，音声指示した頭文字で始まる言葉について口頭でなるべく多く答えることを求めることを20秒ごとに3回繰り返す．言語流暢性課題は60秒間で行うことが多いが，20秒ごとに頭文字を変更するのは精神疾患患者でも回答が途切れることを少なくするためである．回答が途切れると，発声がなくなる影響に加えて，被検者が課題の遂行を放棄したかどうかの判別が難しくなってしまう．また，頭文字を音声指示し回答を口頭で求めるのは，課題の負荷を高めるためである．20秒ごとの語数を課題成績として記録する．最後に，「止め，あいうえお」の音声指示により，「あいうえお」を70秒間繰り返す．

光トポグラフィー検査の結果の評価

1．データ解析のための前処理

NIRSデータについては，賦活前後のレベルにより一次補正を行う．ブロック・デザインの測定において，課題により賦活した脳活動が課題終了後しばらくたつと賦活前のレベルに戻ることを仮定した方法である．レーザの特性によりNIRS信号が直流変動することがあるので，それにも対応している．60秒間の言語流暢性課題の開始前−10〜0秒区間の10秒間と終了後60〜70秒区間の10秒間をそれぞれ前後のゼロレベルとして一次補正する．

また，移動平均法を用いてNIRSデータを平滑化する．ウィンドウ幅5秒のNIRSデータを

表　NIRSで捉えた精神疾患の前頭葉機能(模式図)

	NIRS波形	賦活反応性
健常者	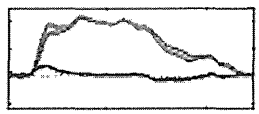	明瞭
うつ病	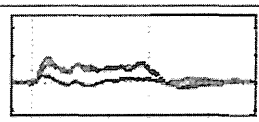	減衰
双極性障害	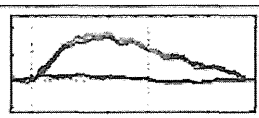	遅延
統合失調症	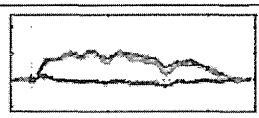	非効率

平均して，ウィンドウ中央の時点におけるNIRSデータとする．アーティファクトなどに基づく高周波数成分を除去する目的としている．

2．視察によるデータの判定(表，図3)

得られたデータのうち特にoxy-Hbに注目し，その波形データを視察により検討し，また補助としてトポグラフィー表示を参考にする．注目するのは前頭部から得られるデータで，①全体的な賦活の大きさ(積分値)，②課題全体を通じた賦活のタイミング(重心値)，③課題初期の賦活のスムーズさ(初期賦活)，の3点についてである．

前頭部における賦活が大きい場合には，前頭葉の賦活反応性が十分であることを示し，気分障害や統合失調症の状態にはない可能性を示唆する．うつ状態の双極性障害では賦活が大きいこともあるが，この後に述べるピークが後半となることが多い．

前頭部における課題全体を通じた賦活のタイミングとは，賦活の大きい時点が課題前半/課題後半/課題終了後のいずれかという点である．波形が滑らかな場合にはピークとして認められるが，波形が不規則な場合にはピークとして捉えにくいこともある．健常者では，課題前半から課題中盤にピークを認めることが多い．ピークが課題終了前後あるいは課題終了後にあったり，あるいはピークが明瞭でなく課題終了前後や課題終了後の賦活が大きい場合は，統合失調症や双極性障害であることが多い．

課題初期の賦活のスムーズさは，波形の最初の部分の傾き(立ち上がり方)として表れる．うつ病では賦活の大きさは小さくても，この部分の傾きは速やかであることが多いので，細かな観察が重要である．この傾きが小さく全体の賦活も小さい場合には統合失調症を，傾きは小さいが賦活の増加が緩やかに続いて全体として大きい場合には双極性障害を考える．双極性障害の躁状態では，この傾きが急峻だが間もなく低下してしまうパターンを示すことがある．

3．自動解析の試み(図4)

上記の結果は各疾患についての群平均データの特徴をもとにした判定であるが，個別データについて定量的で自動的な特徴抽出の試みを進めている．具体的には，①前頭前野背外側面にほぼ対応する前頭部11チャンネルの平均波形を算出し，②得られたoxy-Hb平均波形について，課題区間におけるoxy-Hb増加の累積(積分値)と課題開始前～課題終了後の区間におけるoxy-Hb増加の時間軸上の中心位置(重心値)の2パラメータを自動抽出し，③積分値と重心値の2パラメータの組み合わせにより，波形パターンを5分類する，という手順である．

二つのパラメータのうち，積分値は脳賦活の大きさを表す指標である．光路長の個人差や部位差があるため，チャンネル間の平均波形を求めることや個人間で比較することは望ましくないとされるので，それを含んだ一つの近似値としての指標である．もう一つの重心値は，脳賦活のタイミングを表す指標であり，時間分解能が高いNIRSの特徴を生かした指標である．この2指標を用いると，波形を5パターンに分類でき，この5パターンが疾患ごとに異なる分布を示すという予備的な結果を得ている．

こうしたパラメータの自動抽出に基づく解析においては，①複数チャンネルを平均した波形に基づくもので，チャンネルごとの波形の相違を考慮していない，②上記の二つのパラメータ以外の特徴を考慮していないなどのことがあるため，視察判定を併用することで疾患ごとの特徴をより捉えやすくなる印象がある．

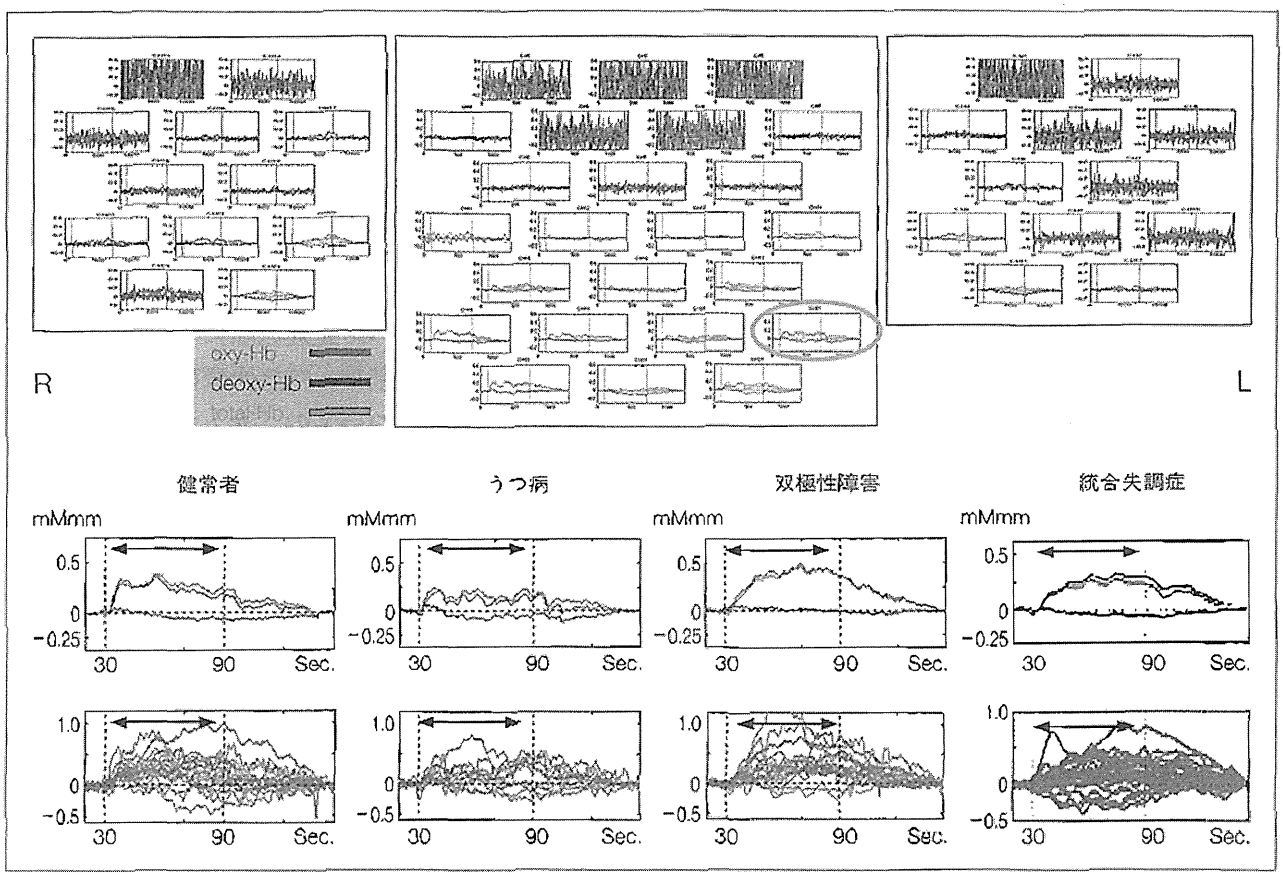

図3　NIRS で捉えた精神疾患の前頭葉機能

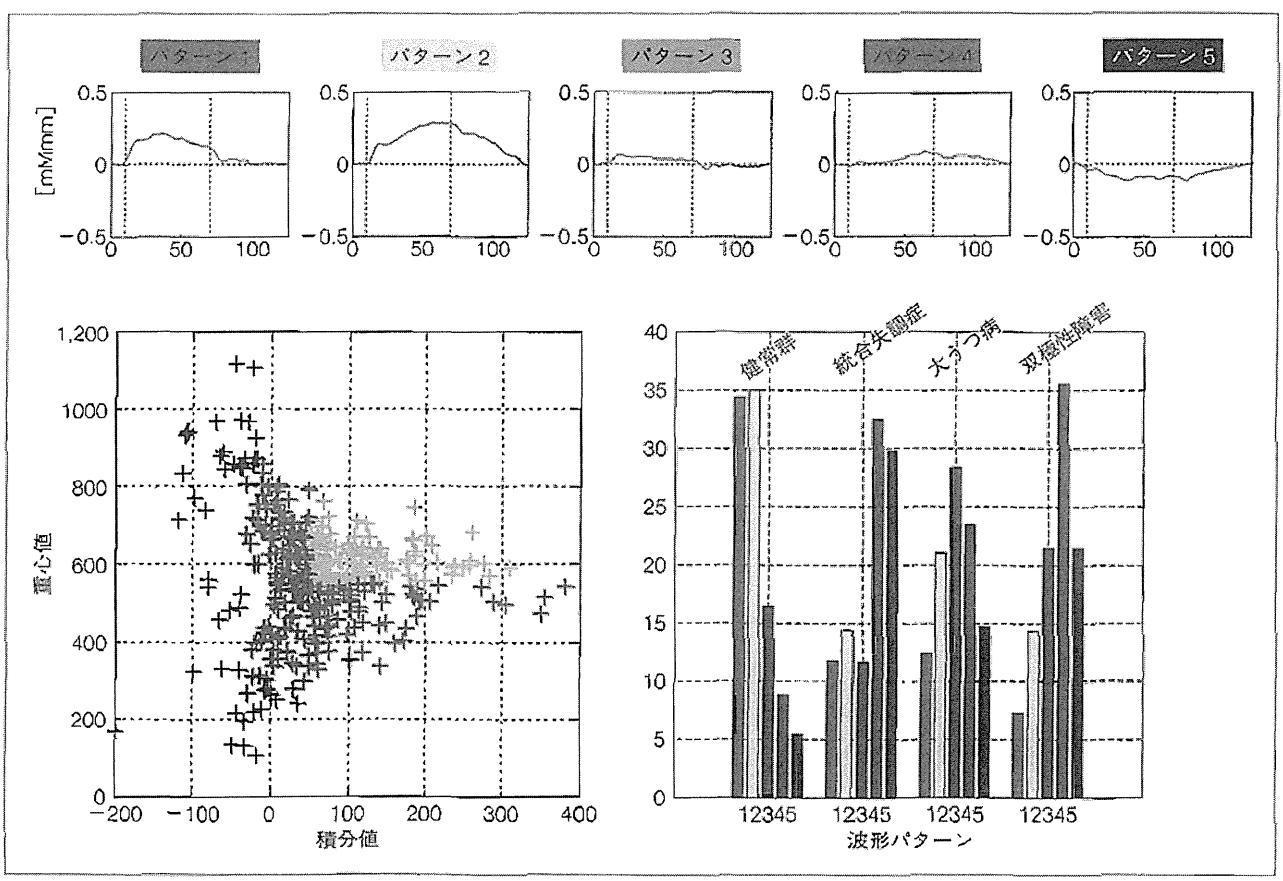

図4　NIRS データの自動解析と疾患ごとの分布

精神疾患のための臨床検査

1．精神疾患の診断の現状

精神疾患は予想以上に多い疾患である．認知症や統合失調症を除いても，わが国の一般人口における精神疾患の1年有病率8.8%，生涯有病率24.4%という報告がある．生命に及ぼす影響や障害の原因としても重要で，WHOが用いている障害調整生命年(disability-adjusted life years, DALY)を指標にすると，わが国では精神神経疾患がその20.7%を占め第1位で，悪性新生物や循環器疾患を上回っている．医療機関を受診する患者はその一部にすぎないが，厚生労働省の患者調査ではわが国の受診患者数は149万人(1990年)→218万人(1996年)→258万人(2002年)→323万人(2008年)と増加を続けている．そのため2011年には，癌・脳卒中・急性心筋梗塞・糖尿病とならび，医療法に基づいて厚生労働省が定める5大疾病の一つに指定された．

こうした精神疾患の診断や治療は，主に臨床症状と病歴とに基づいて行われており，多くの精神疾患の診断や治療に有用な臨床検査は現在のところ確立されていない．そのため，一般外来を受診する患者における精神疾患についての内科医と精神科医の診断一致率は19.3%に過ぎず，患者5人のうち4人は見逃されるか誤診されているという現状がある(WHO調査)．また，臨床検査が未確立であることが，予防や早期診断を困難にしている側面がある．

2．精神疾患のための臨床検査の意義

脳画像検査法の進歩などにより精神疾患における脳の微妙な変化が捉えられるようになり，脳科学の対象が「理性脳→感情脳→社会脳→自我脳」と精神疾患に近づいてきたことなどから，今後は精神疾患についての臨床検査の実現が期待されている．NIRSのような検査で「こころの病を目に見えるようにする」ことは，問診に基づく診断や治療の客観性や確実性や定量性を高めるための補助検査として医療者にとって役立つばかりでなく，そのデータを当事者や家族にも見てもらうことで，当事者中心の精神科医療を進めるうえでも有用と考えられる．

なお，本稿で述べた先進医療についての研修の機会として，国立精神・神経医療研究センター病院が，検査技術についての「光トポグラフィー講習会」と，データ判読についての「光トポグラフィー判読セミナー」を開催している．また，NIRSによる脳機能測定の情報交換の場として日本光脳機能イメージング研究会があり，毎年200名以上の参加者がある(http://jofbis.umin.jp)．

謝　辞

原稿に貴重なコメントをいただきました群馬大学医学部附属病院検査部の臨床検査技師の皆さんに深謝いたします．

参考図書

【NIRS全般について】

酒谷薫：NIRSの基礎と臨床．新興医学出版，2012

【精神疾患におけるNIRSについて】

福田正人：精神疾患とNIRS—光トポグラフィー検査による脳機能イメージング．中山書店，2009

【先進医療としてのNIRSについて】

福田正人：NIRS波形の臨床判読—「うつ症状の光トポグラフィー検査」ガイドブック．中山書店，2011

【精神疾患の脳画像検査について】

福田正人：精神疾患と脳画像．中山書店，2007

Spontaneous slow fluctuation of EEG alpha rhythm reflects activity in deep-brain structures: A simultaneous EEG-fMRI study

Kei Omata[1,2,5], Takashi Hanakawa[3,4], Masako Morimoto[1,5], Manabu Honda[1,5]

[1]Department of Functional Brain Research, National Institute of Neuroscience, National Center of Neurology and Psychiatry, Kodaira, Tokyo, Japan

[2]Department of Biofunctional Imaging, Medical Photonics Research Center, Hamamatsu University School of Medicine, Hamamatsu, Shizuoka, Japan

[3]Integrative Brain Imaging Center, National Center of Neurology and Psychiatry, Kodaira, Tokyo, Japan

[4]Japan Science and Technology Agency, PRESTO, Saitama, Japan

[5]Japan Science and Technology Agency, CREST, Saitama, Japan

Corresponding author: Manabu Honda

4-1-1 Ogawa-Higashi, Kodaira, Tokyo 187-8502, Japan

Department of Functional Brain Research, National Institute of Neuroscience, National Center of Neurology and Psychiatry, Tokyo, Japan

E-mail: honda@ncnp.go.jp; Tel: +81-42-346-1718; Fax: +81-42-346-1748

Abstract

The emergence of the occipital alpha rhythm on brain electroencephalogram (EEG) is associated with brain activity in the cerebral neocortex and deep brain structures. To further understand the mechanisms of alpha rhythm power fluctuation, we performed simultaneous EEGs and functional magnetic resonance imaging recordings in human subjects during a resting state and explored the dynamic relationship between alpha power fluctuation and blood oxygenation level-dependent (BOLD) signals of the brain. Based on the frequency characteristics of the alpha power time series (APTS) during 20-minute EEG recordings, we divided the APTS into two components: fast fluctuation (0.04-0.167 Hz) and slow fluctuation (0-0.04 Hz). Analysis of the correlation between the MRI signal and each component revealed that the slow fluctuation component of alpha power was positively correlated with BOLD signal changes in the brain stem and the medial part of the thalamus and anterior cingulate cortex, while the fast fluctuation component was correlated with the lateral part of the thalamus and the anterior cingulate cortex, but not the brain stem. In summary, these data suggest that different subcortical structures contribute to slow and fast modulations of alpha spectra on brain EEG.

Introduction

Spontaneous electroencephalogram (EEG) is widely used as a clinical tool to judge the general condition of the brain, such as the stage of sleep or level of consciousness. The EEG rhythm that ranges from 8 to 13 Hz when recorded from the occipital area during a resting state with the eyes closed is termed the alpha rhythm [1] or posterior dominant rhythm. The alpha rhythm is generally considered an index of vigilance or arousal, and the emergence of alpha oscillations is thought to represent an "idling" state of the relevant cortices [2,3]. In addition, the alpha rhythm is now widely used as an index of evaluation for relaxation or pleasure in various fields such as neuromarketing [4-6].

Previous studies using multimodal methods, especially simultaneous EEG recordings and neuroimaging procedures, have attempted to identify the areas of the brain correlated with the power of the alpha rhythm [7-17]. In general, negative correlations between alpha power and brain activity have been reported within the cerebral neocortex, especially the occipital, parietal, and inferior frontal regions, whereas positive correlations have been observed within the central deep-lying brain regions such as the thalamus, amygdala, and insula as well as the anterior cingulate cortex and cerebellum.

The negative correlation between cortical activation and the EEG in the alpha frequency range is a relatively common finding across previous studies. It is well established that the power of the alpha rhythm decreases when cortical activity beneath the EEG electrode increases, including alpha attenuation [1] and event-related desynchronization (ERD) [18]. Recently, this relationship was applied to the field of brain–machine/computer interface (e.g. [19]). Conversely, positive correlations between the alpha rhythm and brain activity by fMRI are not always reported and the causes remain unclear, which may be partly due to inaccuracy in the assumption of a fixed canonical HRF as shown by De Munck et al. [20,21].

The spontaneous fluctuation of alpha power is likely to reflect a mixture of multiple factors, each having a different dynamic characteristic. First, the generation and modulation of alpha rhythm is thought to involve different brain regions. Salek-Haddadi et al. [22] reported that "alpha oscillations may be related to three different types of areas: (1) the generators of the cortical rhythm, such as the occipital cortex; (2) areas forming part of the circuit but not directly generating the scalp-detectable rhythms (e.g. thalamus); and (3) other areas correlated with alpha but not causally linked, for example as linked to changes in arousal only." Second, the transition of alpha oscillation has some different dynamics. For example, a phenomenon known as "waxing and waning" of the alpha rhythm occurs for a period of several seconds [23]. Moreover, the ERD occurs within seconds after stimuli [3]. Furthermore, the arousal level characterized by alpha oscillation [24] is altered very slowly and has a longer time constant.

Thus, if different brain systems regulate alpha rhythm in parallel, the alpha power time series (APTS) on EEG may consist of different dynamic components of alpha power. To test this hypothesis, we performed simultaneous EEG and fMRI to record the alpha oscillation and brain

activity during a resting state. By applying a data-driven method known as empirical mode decomposition (EMD) [25] and low and high pass filters to EEG data to separate the APTS into several components, we examined the relationship between the different frequency components of the alpha power time series (APTS) on EEG and brain activity to determine the dynamics of the relevant brain regions in alpha power fluctuation.

In the present study, we focused on the positive correlation between the alpha rhythm and brain activity for practical use of EEG signals to monitor activity in deep-lying brain regions. These regions of the brain are known to be involved in diffuse regulation by means of widely modulating neuronal responses through diffuse projections from the brain stem to various parts of the brain, such as the reticular formation [26]. By determining the relationship between EEG signals and deep-lying brain region activity, scalp EEG may be used as a practical index of activity of deep brain structures without functional magnetic resonance imaging (fMRI).

Materials and Methods

Subjects

Twenty healthy volunteers participated in this study (9 female and 11 male subjects; mean age, 27.3 years). The subjects gave written informed consent before the experiments, which were approved by the institutional ethical review board of the National Institute of Neuroscience, National Center of Neurology and Psychiatry. According to the approved protocol, subjects with a current or previous history of neurological or psychiatric disorders and those with metal implantation were excluded from the study. The subjects were asked to lie still on a scanner bed in the dark for 20 minutes with their eyes closed, but not fall asleep, to obtain spontaneous variations in the alpha rhythm.

Measurements of simultaneous EEG and fMRI

EEGs were recorded with a 32-channel MR-compatible EEG amplifier (Brain Products, Munich, Germany) and an EEG cap with Ag/AgCl electrodes according to international standards (10/20 system). To correct ballistocardiogram artifacts, electrocardiographic data were also captured from electrodes on the backs of subjects. The reference electrode for the EEG recording was positioned between Fz and Cz. EEG data were acquired at a rate of 5 KHz using BrainVision Recorder software (Brain Products). The EEG amplifier had an amplitude resolution of

16 bits. A vacuum cushion was used to fix the subject's head within the head coil to avoid artifacts originating from subject movement and the ballistocardiogram [c.f.] [27]. The amplifier system was placed beside the subject's head within the scanner during fMRI to shorten the cable between the EEG cap and the amplifier.

MRI was performed with a 3-Tesla scanner (Trio; Siemens, Erlangen, Germany) using a standard transmitter-receiver coil. The T1-weighted sequence, MPRAGE, was used for anatomic referencing of the fMRI recordings and co-registration (TR, 2000 ms; TE, 4.4 ms; FA, 80 degrees; voxel size, 1 × 1 × 1 mm; 196 slices). For functional scans, T2*-weighted, gradient-echo, echo planar imaging was used (TR, 3000 ms; TE, 30 ms; FA, 90 degrees; voxel size, 3 × 3 × 3 mm; 40 slices). A total of 404 image volumes were acquired at the rate of one every 3 seconds. The first four volumes were discarded to avoid magnetic saturation effects. The total time per session was 20 minutes.

To establish time alignment between the EEG data and blood oxygenation level-dependent (BOLD) signals, a SyncBox device (Brain Products) was used to achieve phase synchrony between the clock for digital sampling of the EEG data and that for driving the MR systems gradient switching. Thus, the starting point of MR image acquisition in each interval was marked in the EEG time course data in which data sampling points were precisely synchronized with MR image acquisition. These markers were used for MRI scanner artifact correction, as described below.

Analysis of EEG data

To correct artifacts originating from the MRI scanner and ballistocardiogram, the recorded EEG data were processed by BrainVision Analyzer 2.0 (Brain Products) using the average template subtraction method [28,29]. First, all data were filtered by a low-pass filter with a cut-off frequency of 70 Hz. Because MRI scanner artifacts were regularly repeated every TR interval, the interval of these artifacts could be precisely identified from the markers of the starting point of each MR image acquisition. A template of MRI scanner artifacts in EEG signals was created by averaging the MRI scanner artifacts over a set number of intervals and subsequently subtracting this average from the data. The sampling rate of the data was decreased to 250 Hz. Second, the ballistocardiogram artifacts were removed in a similar fashion. The peaks of the R-waves detected in the electrocardiographic channel were marked by a cross-correlation between a semi-automatically defined pulse peak and the data. A template was created by averaging the EEG data time-locked to the timing of the detected R-wave peaks, and then the averaged template was subtracted from the original EEG data for each R-wave peak. We also employed an independent component analysis (ICA) [30,31] and obtained a similar result. This

compared well with a report by Grouiller et al. [32] showing that the template subtraction method is efficient in removing artifacts for experimental data.

To avoid bias effects from the reference positions (e.g., TP9, TP10, FCz), and to specify the alpha power of the parieto-occipital regions, the corrected EEG data recorded from the parieto-occipital regions (i.e., P3, P4, P7, P8, O1, and O2 in the international 10/20 system) were reconfigured into four bipolar derivations (i.e., P7-O1, O1-P3, P8-O2, and O2-P4) after correction of the MRI scanner and ballistocardiogram artifacts. The re-reference to the parieto-occipital regions emphasizes the relevant local EEG sources over global EEG sources by removing signals that are common between the neighboring electrodes. The data were segmented every 3 seconds to match the TR of the fMRI data. The powers of the frequency components in these four channels were calculated by fast Fourier transformation (FFT) with a frequency resolution of 0.5 Hz. A moving time window of 2-second lengths with interpolation was used to calculate the FFT of 3-second analysis epochs to ensure the alpha frequency range from 8 to 12.5 Hz. The powers of the alpha rhythm band (8–12.5 Hz) for each channel were averaged for each segment. Averaging the powers across hemispheres emphasizes or assumes commonality in this measure across hemispheres. This procedure resulted in an average alpha band power every 3 seconds, denoted as the APTS (Figure 1A). The data points in the APTS exceeding the standard deviation by 3-fold or greater were excluded and replaced by linearly interpolated values. To exclude systematic differences in the amplitude of the APTS across subjects, the APTS in each subject was normalized to the range of 0 to 1, as follows [33]:

$$Normalized\,APTS = (Original\,APTS - APTS\,\min)/APTS\,\max$$

Here, APTSmin and APTSmax represent the minimum and maximum values of APTS, respectively. The original APTS was used as a regressor in the general linear model (GLM) for fMRI analysis to explore the brain regions whose activity specifically correlated with the original APTS. We assumed that the APTS may reflect a different type of brain mechanism of generation or modulation of the alpha EEG. To examine for such a mechanism, we focused on the dynamic aspect of the APTS changes and analyzed the frequency components of the APTS. To divide the APTS into sub-frequency components, a data-driven method termed empirical mode decomposition (EMD) introduced by Huang et al. [25] was employed. The EMD is an algorithm whereby a single time-course is decomposed into its oscillatory components and is applied to non-stationary and nonlinear time series analysis [25], such as APTS and BOLD signals. For example, Niazy et al. [34] reported the ability of the EMD for investigating time series of spontaneous BOLD signals during resting-state. Each oscillatory component is called an intrinsic mode function (IMF) that is defined by the following two conditions. First, the number of zero-crossings and extrema must be the same or differ at most by 1. Next, the mean between the upper and lower envelopes must be close to zero according as stopping criteria.

The algorithm of EMD [35] can be described as follows:

Given a signal $x(t)$,

1. Identify all extrema of $x(t)$
2. Interpolate between minima (resp. maxima), resulting in an envelope $e_{min}(t)$ (resp. $e_{max}(t)$)
3. Compute the mean $m(t) = (e_{min}(t) + e_{max}(t))/2$
4. Extract the detail $d(t) = x(t) - m(t)$
5. Iterate on the residual $m(t)$

Steps 1 to 4 are iterated until the detail satisfies the above two conditions. This procedure is defined as a sifting process [25,35,36]. The detail is referred to as an IMF after the sifting process stops, the residual is calculated, and step 5 is followed.

The APTS was subjected to the EMD algorithm to explore its IMFs. Figure 1B depicts the application of the EMD to the APTS of a single subject. In the present study, we chose IMFs 1 to 5 for further analyses. The IMFs were subjected to FFT analysis to explore the frequency profile. The Nyquist frequency of the FFT was 0.167 Hz as the APTS was sampled every 3 seconds. Figure 2A depicts all the spectrums of the IMFs of each subject. Each IMF group derived from different subjects roughly covered the same frequency band (Figure 2A). Figure 2B shows the averaged power spectrums of each IMF across all subjects. It is worth noting that each IMF has a unique frequency band (the first IMF covers the highest frequencies and the last IMF covers the lowest one), and that each frequency band of the IMFs have crossovers with each other. These IMFs were used as regressors in the GLM for fMRI analysis to explore the brain regions whose activity specifically correlated with each IMF.

According to the results of the correlation between the IMFs and brain activity, to verify the results we divided the APTS into slow and fast fluctuation components of the APTS using low and high pass filters. Based on the crossover between the averaged power spectrum of IMF2 and IMF3, the two fluctuation components of the APTS were defined as follows: slow fluctuation(<0.04 Hz) and fast fluctuation (>0.04 Hz) (Figure 2B). Each fluctuation component was then extracted by filtering the original APTS with Butterworth low-pass and high-pass filters (low-pass filter: passband ripple, 3 dB; passband frequency, 0.04 Hz; slope, -49 dB per octave; high-pass filter: passband ripple, 3 dB; passband frequency, 0.04 Hz; slope, 48 dB per octave). These two fluctuation components were used as regressors in the GLM for fMRI analysis to explore the brain regions whose activity specifically correlated with each fluctuation component, as described below. Note that the slow and fast APTS components and the slow (8–10 Hz) and fast (10–13 Hz) alpha rhythms should be not be confused with each other. The fast alpha rhythm refers to the frequency components of the raw EEG waveform, while the slow alpha rhythm refers to the frequency components in the longer trend of the power of

the alpha frequency band of the EEG.

Analysis of fMRI data

fMRI data were analyzed with SPM5 on MATLAB (MathWorks, Natick, MA, USA). Preprocessing of the fMRI included slice timing correction, realignment, spatial normalization, and spatial smoothing with an 8-mm, three-dimensional Gaussian filter [37]. The brain regions whose BOLD signals were correlated with the EEG components, namely the APTS and each of its components, were statistically evaluated with a general linear model [37] in which both the explanatory variables of interest and those of non-interest were used as multiple regressors. Each original APTS, its IMFs, and its slow and fast fluctuation components were convolved with the canonical hemodynamic response function to take into account hemodynamic delay and dispersion of BOLD signals, and then used as an explanatory variable. The six realignment parameters were used as variables of non-interest to remove the effect of head motion on MRI signals. The MRI signal of cerebrospinal fluid (CSF) was also used as an explanatory variable of non-interest to exclude signals originating from vessels and ventricular areas reflecting cardiac beats and respiration [38-40] that were irrelevant to the neural activities. The CSF signal was calculated by averaging the MRI signal in the ventricles, which were anatomically defined by the segmentation function of SPM5. When taken together, we conducted three types of GLM, with (i) the GLM of the original APTS, (ii) its IMFs, and (iii) its slow and fast fluctuation of the APTS, estimated separately. Each GLM included the six realignment parameters and the CSF signal as nuisance covariates.

For each GLM, at the first level the contrast images corresponding to the regressors were created for each subject and entered into a second level one-sample t test. Additionally, for the third GLM, a paired t test was conducted to determine whether the contrast weights were significantly different between the slow and fast fluctuation components within regions of interest inclusively masked by brain regions that positively correlated with either the slow or fast fluctuation components. For all data, a threshold of uncorrected $p < 0.001$ for peak-level and a cluster-level family-wise error (FWE) of 0.05 [41] were used for statistical analyses. An atlas of the human brain was used as an anatomical reference for the deep-lying brain regions [42].

Results

In this manuscript, we use the term "correlation" to explain the relationships between the

explainable values and the brain activity in the GLM. The original APTS was positively correlated with brain activity in the thalamus, anterior cingulate cortex, brain stem, and cerebellum and was negatively correlated with activity in the broad areas of the cerebral cortex (the superior parietal lobule, cuneus, middle occipital gyrus, middle frontal gyrus, rectal gyrus, and inferior temporal gyrus) (uncorrected $p < 0.001$, extent > 103 voxels) (Figure 3, Table 1). These findings are generally concordant with those of previous reports [7,11,12,15-17].

Figure 4 illustrates the brain regions with activities that correlated with the IMFs. Tables 2 and 3 show the details of the positive and negative correlated areas, respectively. While the threshold of uncorrected $p < 0.001$ for peak-level was used, the extent threshold that was equal to a FWE of 0.05 was different from each IMF (IMF1: extent > 96; IMF2: extent > 130; IMF3: extent > 114; IMF4: extent > 166; IMF5: extent > 128). The results of the positive correlation with the IMFs are shown in the upper part of Figure 4. The IMF1 was correlated with activity in the anterior-lateral part of the thalamus, the anterior cingulate cortex, the dorsolateral prefrontal cortex, the cerebellum, and the caudate nucleus. Similarly, the IMF2 was correlated with activity in the anterior cingulate cortex and the anterior part of the thalamus. Conversely, the IMF3 was correlated with activity in the medial part of the thalamus and the brain stem. The IMF4 was correlated with activity in the medial dorsal part of the thalamus. Furthermore, the IMF5 was correlated with activity in the lateral and medial part of the thalamus and brain stem (Figure 4 and Table 2). In summary, both IMF1 and 2, including the higher frequency band of the APTS, were positively correlated with brain activity in the anterior cingulate cortex and the anterior-lateral part of the thalamus, whereas the IMF3, 4 and 5, including the lower frequency band of the APTS, were positively correlated with brain activity in the medial-dorsal part of the thalamus and/or the brain stem.

The results of the negative correlation with the IMFs are shown in the bottom part of Figure 4. The negative correlation with each IMF component was found within the occipitoparietal cortex, but not in all the IMF components. Although the results of the IMF1 and IMF2 showed a small amount of negative correlation in the brain regions, IMF3, 4, and 5 were widely negatively correlated with activity in the occipital-parietal cortex. The IMF1 was correlated with activity in the left inferior frontal cortex, and the IMF2 was correlated with activity in the superior parietal lobe and precentral gyrus. Subsequently, the IMF3 was correlated with activity in the occipitoparietal cortex, the inferior frontal cortex, the orbitofrontal cortex, and the middle temporal gyrus. The IMF4 was correlated with activity in the occipitoparietal cortex, the inferior temporal gyrus, and the inferior frontal gyrus. Furthermore, the IMF5 was correlated with activity in the middle occipital gyrus, the precentral gyrus, the medial temporal pole, and the middle orbital gyrus (Figure 4 and Table 3).

More importantly, the slow and fast fluctuation components of the APTS showed a specific relationship with brain activity (uncorrected, $p < 0.001$ and extent > 131 voxels

for the slow fluctuation and 75 voxels for the fast fluctuation, respectively). Figure 5 illustrates the brain regions with activities that correlated with either slow or fast fluctuation. Table 4 gives details of the correlated areas. Slow fluctuation was correlated with activity in the medial part of the thalamus and brain stem, the anterior cingulate cortex, the amygdalae, and the cerebellum. By contrast, the fast fluctuation component was correlated with activity in the cerebellum, the anterior and middle cingulate cortex, the superior frontal cortex, and the lateral part of the thalamus.

A comparison between the brain regions positively correlated with the slow and fast fluctuation components (slow > fast) also revealed a significant difference between components in the middle part of the thalamus and the brain stem (Figure 6 and Table 4, uncorrected $p < 0.001$, extent > 135 voxels). Conversely, there was no significant difference in the comparison between the fast and slow fluctuation components (fast > slow).

Discussion

We conducted simultaneous EEG/fMRI recordings to examine the dynamic relationship between alpha power of EEG and brain activity. We found that the slow and fast fluctuation components of the APTS were correlated with different brain regions in the thalamus, anterior cingulate cortex, and brain stem. These data generally agrees with our hypothesis that the APTS contains mixed dynamics of the alpha power, and suggests that different brain systems may regulate alpha rhythm in parallel.

Brain regions associated with IMFs of the alpha EEG

We applied the EMD to the APTS to separate it into five IMF components (Figures 1 and 2). In the fMRI analysis, the brain regions positively correlated with each IMF must be categorized into two types of relevant brain regions (see Figure 4 and Tables 2 and 3). The first type mainly consisted of the anterior cingulate cortex and the anterior and lateral part of the thalamus (the results of the IMF1 and 2). The second type predominantly involved the medial and dorsal part of the thalamus and the brain stem, (the results of the IMF3, 4 and 5). The negative correlation between the activity and the IMFs was also categorized into two types. The results of the IMF1 and 2 showed almost no significant brain regions, while that of the IMF3, 4, and 5 showed significant brain regions spreading over the occipital and parietal cortex (see Figure 4). Taken

together, these data suggest that the IMF1 and 2 of the APTS are qualitatively different from the IMF3, 4, and 5. There were noticeable differences between the two IMF groups with regard to the thalamus, the anterior cingulate, and the brain stem, supporting the hypothesis that different brain systems may be regulating alpha rhythm in parallel.

Interestingly, the IMF3, 4, and 5 showed no correlation with the activity in the ventral anterior cingulate (vACC), whereas the slow fluctuation of the APTS that corresponded to the IMF3, 4, and 5 explained the brain activity in the vACC (Figures 4 and 5). Thus, the activity in the vACC must include the broad frequency component extending in the range 0–0.04 Hz.

Brain regions associated with slow and fast fluctuations of the alpha EEG

Our results suggest that the correlation between brain activity and the IMFs must be categorized into two types. The brain regions that correlated with the IMF1 and 2 were noticeably different from that of the IMF3, 4, and 5. Furthermore, the profiles of the power spectrums of the second and the third components had an obvious crossover at 0.04 Hz (see Figure 2B and Figure 4). Therefore, we separated the APTS into slow and fast fluctuation components using a low and high pass filter at 0.04 Hz. Fast fluctuation corresponded to instantaneous increases and decreases in alpha power oscillation, while slow fluctuation corresponded to slower changes depending upon the prominence of alpha oscillation. In the fMRI analysis, the brain regions that correlated with slow and fast fluctuations differed from each other (Figure 5). There were noticeable differences among the thalamus, anterior cingulate cortex, and brain stem, supporting the notion that the brain regions involved in alpha rhythm generation and those indirectly affecting alpha rhythm might coexist and modulate alpha oscillation independently.

Salek-Haddadi et al. [22] stated that "alpha oscillations may be related to three different types of areas: (1) the generators of the cortical rhythm, such as the occipital cortex; (2) areas forming part of the circuit but not directly generating the scalp-detectable rhythms (e.g. thalamus); and (3) other areas correlated with alpha but not causally linked, for example as linked to changes in arousal only." Brain regions with activity that is positively correlated with fast fluctuation of the alpha rhythm may be located in the lateral part of the thalamus, which is thought to form the thalamocortical circuit that generates the alpha rhythm [43]. These regions may correspond to the second mechanism proposed by Salek-Haddadi et al. [22]. The brain regions that are positively correlated with slow fluctuation may indirectly affect the generation of alpha oscillations through slow changes in brain states, corresponding to the above-mentioned third mechanism.

The arousal level plays an important role in the emergence of the alpha rhythm. Traditionally, the existence of alpha and beta

oscillations on the EEG has indicated a wakeful state (e.g. [24]). Therefore, the positive correlation between brain activity and the slow fluctuation of the APTS may reflect the arousal level. In fact, the brain stem and medial part of the thalamus, the activity of which were correlated with slow fluctuation, form part of the reticular formation that is associated with the arousal level [26]. In the present study, we evaluated the arousal level of the subjects during the experiment using a traditional method [24] (data not shown) and found that the experimental period comprised both awake and drowsy states. Regarding cortical activity during the drowsy state, Horovitz et al. [44] showed increased BOLD fluctuations in the visual cortex during light sleep. We found a negative correlation between the slow fluctuation of the APTS and the occipital-parietal cortex, as the alpha power decreases during the drowsy state. These evidences suggest that the decrease of alpha power during drowsy state may reflect the increase of BOLD signal fluctuations.

In addition to the arousal level, we considered another possibility for the involvement of monoaminergic neurons in the brain stem. The efferent nerves of the monoaminergic systems convey impulses from the brain stem to broad areas of the cerebral cortex [2,26,45,46]. The cortical state changed by monoamine neurotransmitters can occasionally be maintained for seconds to minutes (e.g. [47-51]). Considering the time scale of the slow fluctuation component of the alpha power, in which the frequency is below 0.04 Hz (i.e., a period of time longer than 25 seconds), we suggest that this component may also reflect the activity of the diffuse modulator system in the brain stem.

Most monoamine neurons project from the brain stem structures to diffuse brain areas: dopamine from the ventral tegmental area and substantia nigra of the midbrain; serotonin from the raphe nuclei extending throughout the medulla, pons, and midbrain; and noradrenaline from the locus coeruleus in the rostral pons [52]. Although the relevant activation cluster in the brain stem was mainly located in the ventral part of the midbrain and the rostral pons, it is difficult to infer which of the monoamine transmitters might be responsible as the monoamine neurons have reciprocal interactions. However, the cluster explored in the present study is likely to cover these structures.

The positive correlation between the activity in the brain stem and the slow fluctuation, but not the fast fluctuation, suggests that the slow fluctuation may be useful as an index of brain activity in the brain stem. For instance, activity in certain areas of the brain stem, such as the raphe nucleus, is correlated with symptoms of depression [53]. Thus, scalp EEG signals may be useful as biomarkers for such psychiatric symptoms through indirect monitoring of brain stem activity, including that in the raphe nucleus.

The regions of the thalamus that are correlated with slow fluctuation are thought to include the nuclei situated in the dorsomedial part. These nuclei are likely considered to be part of a nonspecific projection system and have a functional role in modulating the degree of activity in the cerebral neocortex [54]. By contrast, regions that are correlated with fast fluctuation are

situated more laterally (Figure 5) and are likely to include nuclei with specific projections to the cerebral neocortex and form a thalamocortical loop involved in the generation of alpha oscillations [26,43,54]. Furthermore, Schreckenberger et al. [55] reported that the activity of the lateral part of the thalamus was tightly coupled with the alpha power under lorazepam treatment in a PET/EEG study. In that study the correlation of the alpha rhythm to thalamic activity was suggested to reflect thalamic generation of cortical alpha power by the changing of firing patterns in the lateral thalamic nuclei. The coordinates of the lateral thalamus nuclei seem close to the regions that correlated with the fast fluctuation in the present study.

In the present study, the particular regions that were correlated with the fast fluctuation components in contrast to the slow fluctuation components were the superior frontal cortex, and the cerebellum (Figure 5). We believe that the cortical regions in the frontal cortex might be involved in the thalamocortical circuit because of their direct connection with the thalamus [43,56,57]. A conclusion is more difficult to reach in terms of the cerebellum, although it is possible that the correlation between the fast fluctuation and the activity in the cerebellum might reflect activity of cerebrocerebellar interaction, as the cerebral cortex and cerebellum have a crossed connection and the regions in the cerebral cortex and cerebellum illustrated in the present study were lateralized to the right and left, respectively. Of course, these interpretations should be explicitly tested in the future.

The cingulate cortex has a direct connection with various thalamic nuclei [58-60]. Although it was difficult to precisely identify the thalamic nuclei in detail using the low spatial resolution of the present study, we believe that the differential involvement of the fast and slow components in the cingulate cortex might reflect differences in thalamic connections. Furthermore, the slow and fast fluctuation components were associated with the brain activity in the dorsal and ventral part of anterior cingulate cortex (dACC/vACC), respectively (Figure 5). The dACC is considered to be involved in cognitive processes, while the vACC in emotional regulation [61,62]. This implies that the fast fluctuation of the APTS may be associated with cognitive processes, and the slow fluctuation may be relevant to emotional processes.

Comparison with previous simultaneous recording experiments

The results in Figure 3 are mostly consistent with those of previous studies [7,10-12,15-17]. Although some studies reported no correlation between BOLD signals in the thalamus and alpha oscillations [13,63] and a negative correlation between the glucose metabolic rates in the thalamus and averaged alpha power [8,9], recent studies have generally shown positive correlations between alpha power fluctuation and BOLD signals in the thalamus and negative correlations

in the occipitoparietal cortex.

Characteristics of APTS fluctuations

In the present study, we tried to characterize two different aspects of alpha power fluctuation, that is, the fast fluctuation corresponding to instantaneous increases and decreases in alpha power oscillation, such as waxing and waning [23], and the slow fluctuation corresponding to slower changes depending upon the ease of alpha oscillation. The cutoff frequency between the fast and slow components was determined based on the brain patterns associated with IMFs using the EMD (see Figures 2 and 4). However, since the occupied frequency of each IMF varied across the subjects, the border of the slow and fast components must be considered as a rough indication.

Brain activity in a resting state, with eyes closed or while looking at a fixed point, was recently examined by looking at changes in BOLD signals (cf. [64]). The majority of the studies postulate that BOLD signal fluctuation of the default mode network, including the posterior cingulate cortex and the medial frontal cortex, is in a frequency range of less than 0.1 Hz [64-68]. Niazy et al. [34] reported that resting-state networks are not merely described by slow spontaneous fluctuations (~0.015 Hz), but by broadband processes that indicate temporal coherences across a frequency spectrum, especially in the range of 0.02–0.05 Hz. Interestingly, the frequency range in the present study (<0.04 Hz) is included in that of the default mode network.

In terms of the relationship between spontaneous fluctuation of BOLD signals and EEGs, using a concurrent EEG and fMRI with group independent component analysis, Bridwell et al. [69] reported positive associations with alpha rhythm within the thalamus and medial frontal gyrus, and negative associations between frontal, parietal, temporal, and limbic fMRI regions, and EEG alpha. Furthermore, an MEG study demonstrated that the default mode network was identified using alpha band data [70]. In addition, He et al. [71] reported that the slow cortical potentials measured by electrocorticography in humans show a correlation structure similar to that of the resting state network in BOLD fluctuations. These findings suggest that the brain network affecting alpha rhythm generation and the resting state may share a common fluctuation mechanism.

Although we have discussed the physiological aspects of the APTS and spontaneous BOLD fluctuation, it is unlikely that alpha power fluctuation solely reflects spontaneous fluctuation. In general, the alpha rhythm is changed by spontaneous fluctuation, and both the internal state of subjects and external stimuli. Alpha oscillation was reportedly increased by sounds containing inaudible high-frequency components associated with activation of the deep-lying brain regions, and

both were significantly correlated [10]. Therefore, the slow fluctuation of alpha oscillation may be useful as a convenient objective marker to monitor the deep-lying brain structures, including the brain stem and medial thalamus.

Conclusions

We showed that the dynamics of the alpha power were positively correlated with brain activity in the deep-lying brain regions, the thalamus and brain stem. Moreover, we showed that the slow and fast fluctuation components of the transient alpha power were correlated with particular brain regions (the slow component with the medial part of the thalamus and the brain stem, and the anterior cingulate cortex; the fast component with the lateral part of the thalamus and the anterior and middle cingulate cortex). These results support our hypothesis that the APTS consist of different dynamics of modulation of alpha oscillation, and that different subcortical structures contribute to slow and fast modulations of alpha spectra.

Acknowledgements

We thank K. Kasahara and C. DaSalla for their help with the experiments.